Natural Hazards
and Earth System
Sciences

Open Access

EGU

Discussions

Short-term volcano-tectonic earthquake forecasts based on a MRT algorithm: the El Hierro seismo-volcanic crisis experience

Alicia García[1], Servando De la Cruz-Reyna[2,3], José M. Marrero[4,5], and Ramón Ortiz[1]

[1]Institute IGEO, CSIC-UCM. J. Gutierrez Abascal, 2, Madrid 28006, Spain.
[2]Instituto de Geofísica. Universidad Nacional Autónoma de México. C. Universitaria, México D.F. 04510, México.
[3]CUEIV, Universidad de Colima, Colima 28045, México.
[4]Instituto Geofísico. Escuela Politécnica Nacional. Quito, 1701-2759, Ecuador
[5]Unidad de Gestión, Investigación y Desarrollo. Instituto Geofráfico Militar. El Dorado, Quito, 170413, Ecuador.

Correspondence to: Alicia García (alicia.g@igeo.ucm-csic.es)

Abstract. Under certain conditions volcano-tectonic (VT) earthquakes may pose significant hazards to people living in or near active volcanic regions, especially on volcanic islands; however, hazard arising from VT activity caused by localized volcanic sources is rarely addressed in the literature. The evolution of VT earthquakes resulting from a magmatic intrusion shows some orderly

5 behavior that may allow forecasting the occurrence and magnitude of major events. Thus governmental decision-makers can be supplied of warnings of the increased probability of larger-magnitude earthquakes in the short term time-scale. We present here a methodology for forecasting the occurrence of large-magnitude VT events during volcanic crises; it is based on a Mean Recurrence Time (MRT) algorithm that translates the Gutenberg-Richter distribution parameter fluctuations into time-

10 windows of increased probability of a major VT earthquake. The MRT forecasting algorithm was developed after observing a repetitive pattern in the seismic swarm episodes occurring between July and November 2011 at El Hierro (Canary Islands). From then on, this methodology has been applied to the consecutive seismic crises registered at El Hierro, achieving a high success rate in the real-time forecasting, within 10 day time-windows, of volcano-tectonic earthquakes

15 ## 1 Introduction

Volcano-tectonic (VT) earthquakes are considered to be low-magnitude compared to tectonic earthquakes, even though in some cases (three in the 20th century) they have reached M≥7 (Zobin, 2001). Volcanic earthquakes occurring near active subduction zones, which may often reach magnitudes in the range 4-6, rarely cause the same degree of damage or concern among the population

20 that stronger tectonic earthquakes cause. However, in volcanic regions with low tectonic activity, and consequently with a higher vulnerability to strong ground motions, events exceeding M4 may

produce significant damage. Such a situation may become quite serious when that type of VT activity occurs in volcanic islands with unstable topographies, prone to land-slides, as is the case of El Hierro, the westernmost, youngest ($<$ 2 Ma, Ancochea et al, 1994), and smallest (269 km^2) of the

25   Canary Islands.

In general, earthquake forecasting requires answers to three questions: where, when, and how large? In VT earthquake forecasting, the answer to where is constrained by the extent of the volcanic system. The answer to the second question on timing is related to the onset and evolution of a volcanic crisis. Such crises are generally characterized by VT seismic swarms, lasting an average of

30   5.5 days in the case of El Hierro, concentrated in regions within or around the volcanic system, and generally defined as "a sequence of events closely clustered in time and space" (Benoit and McNutt, 1996). Since such swarms may include events of damaging magnitudes, it is important to detect the non-random components of the swarm evolution, as it contains factors linking different stages of the process that may allow major VT events to be forecast. We assume that such "causal fac-

35   tors" are related to the nature of the magmatic intrusion process at depth that involves an increasing accumulation of localized stress, which produces the VT earthquake when released. In particular, the magmatic intrusions may produce clustered sources of stress in which pressure increases over relatively short time-scales.

We picture the situation at El Hierro as voluminous bodies of dense magma intruding into the

40   mantle under the crust from a deeper magma generation region (Martínez-Arevalo et al, 2013). That magma is dense enough to remain in almost isostatic equilibrium at the base of the crust in a process of magmatic underplating (Leahy et al, 2010). As it evolves under the local conditions at mantle-crust boundary depths, the diffusive assimilation of crustal minerals causes an increase in the magma buoyancy over the time-scale of centuries as the assimilation diffusivity is at least one order of

45   magnitude higher than the thermal diffusivity (McLeod and Sparks, 1998; Portnyagin et al, 2008). The increasing buoyancy causes additional stresses and deformations in the overlying crust. Such processes may induce a causative evolution of the seismicity, reflected as an increased rate of seismic energy release, and a changing distribution in the magnitudes of the VT events, as discussed in the following sections. However, at this point, it is important to note that the analysis of such evolution

50   may enable scientists to forecast the occurrence of major VT events in the short-term time scale; nevertheless, this analysis cannot foretell definitively the occurrence of an eruption, as the magma injection and migration process may never reach the surface (Bell and Kilburn, 2012), although an increase in the probability of such an event must be considered. We present next this methodology, developed and used during the El Hierro volcanic process (2011-2015), which is aimed at detecting

55   the precursory behavior of the seismicity before the occurrence of major, potentially damaging, VT earthquakes.

Natural Hazards
and Earth System
Sciences

Open Access

Discussions

EGU

2 El Hierro volcanic process

The morphology of El Hierro island (27.7^o N; 18.0^o W) has been attributed to a triple volcanic rift with the NE, NW and S axes of these rifts diverging by about 120° from each other (Carracedo et al, 1999). The island landscape displays abundant dikes and fissures (Gee et al, 2001), as well as major landslides (Masson et al, 2002). The subaerial island displays a high concentration of volcanoes with a spatial distribution that may be explained by the model proposed by Stroncik et al (2009), in which the volcanic activity at El Hierro is controlled by a complex array of magma pockets. Magma injections from the pockets through dikes or sills may generate VT seismicity.

In July 2011, a sudden increase of seismicity was detected at El Hierro Island, prompting several Spanish institutions to deploy recording instrumentation. In addition to the official seismic network operated by the Instituto Geográfico Nacional (IGN), in September 2011, the IGEO-CSIC Institute (see authors' affiliations) installed, for research purposes, a seismic network consisting of 3 permanent, real-time, vertical, short-period stations, and 5 similar, temporary, manual-access stations. Seismicity, deformations and diffuse gas emissions increased persistently until October 2011, when a submarine eruption at 27° 37.18' N; 17° 59.58' W was first detected (López et al, 2012; Ibáñez et al, 2012; Prates et al, 2013). The eruptive activity persisted for months, until March 2012. However, neither the seismic activity nor the deformations stopped, and have in fact continued to the time of this submission (García et al, 2014b, a).

The evolution of the seismic activity at El Hierro island for the whole period of unrest (2011-2015) is summarized in Figure 1, in terms of the time distribution of earthquake magnitudes, the number of earthquakes exceeding M1.5 per day, the cumulative number of events, and the cumulative seismic energy released, estimated from the IGN public earthquake catalog (http://www.ign.es/ign/layoutIn/sismoFormularioCatalogo.do as downloaded on 2015-08-29), and from records of the above-mentioned IGEO-CSIC seismic research network. The uncertainties in calculating the duration and magnitude of very low-amplitude signals recorded by the IGEO-CSIC have been treated according to Del Del Pezzo et al (2003).

Figure 2 near here

Inspection of Figure 1 reveals that the seismicity, deformations and eruption evolution observed during the 2011 unrest episode not only is consistent with the model of Stroncik et al (2009) (García et al, 2014b), but it also reveals some other interesting features of the volcanic unrest process dynamics. First, as expected, a marked rise of the VT event occurrence rate preceded the onset of the 10 October 2011 eruption. However, during the continuing seismic unrest, the event rate and the cumulative number of events have also markedly increased before the occurrence of major VT earthquakes. But it is the cumulative release of seismic energy, shown in the uppermost plot of Figure 1, the parameter that best illustrates the precursory character before major VT events. Additionally, the M-T diagram in the lower plot of Figure 1 shows a peculiar behavior. The minimum magnitude rises as the number of higher-magnitude events increases. This may be caused by com-

Natural Hazards
and Earth System
Sciences

Discussions

pleteness fluctuations of the catalog, derived from the difficulties in counting very small events when
95   larger earthquakes are concurrent, or it may be an actual condition related to the physical process
of seismic energy release. Several other cases in which the completeness is maintained at the lowest
measurable value during the duration of the VT swarm suggest that the latter condition may be real.
For example, Benoit and McNutt (1996) report an increase of the minimum magnitude when the
VT activity approaches a mean magnitude 3. Likewise, De la Cruz-Reyna et al (2008) and Hurst
100   et al (2014) report a similar behavior for the VT seismicity of Popocatépetl and Tongariro volcanoes
respectively.

To date, five seismo-volcanic crises or VT earthquake swarms have been identified at El Hierro
(García et al, 2014b, a), showing in all cases an increasing trend of the maximum detected magni-
tudes, as shown in Figure 2. It is significant that the acceleration of the seismic energy release rate
105   begins in all cases when the cumulative seismic energy exceeds the 10^{11}J energy threshold criterion
of Yokoyama (1988). Hours to days after the onset of this acceleration stage, the swarm sequences
culminated with earthquakes exceeding magnitude 4 (Figure 3). Currently, VT earthquake swarms
are classified according to three family types proposed by Benoit and McNutt (1996), and later up-
dated by Farrell et al (2009) and Brumbaugh et al (2014): Type A- mainshock and aftershocks; type
110   B- foreshocks, mainshock and aftershocks; and type C- swarms without a mainshock. Further exam-
ination of the lower part of Figure 2 reveals that the evolution of the daily rate of seismicity does not
correspond to any of these established earthquake families. We thus introduce a fourth family, type
D, characterized by an increasing number of growing magnitude foreshock events culminating with
a mainshock and followed by a rapid decay of seismicity lasting just a few hours. The differences
115   between these models are illustrated in Figure 4. Therefore, a type D sequence does not follows
an ETAS model (Ogata, 1992), nor follows the Omori law (Utsu and Ogata, 1995), but it reveals a
causal process that allows forecasting of major VT events.

Figure 2 near here

Figure 3 near here

120   **Figure 4 near here**

2.1   Forecasting major VT earthquakes at El Hierro

In a time-evolving seismicity, the Gutenberg-Richter Law (GRL, Gutenberg and Richter, 1944)
scales the activity, with respect to its magnitude, as:

Equation 1 here

125   where $N(M)/\Delta T$ is the number of earthquakes with magnitude M or larger detected within a
given region, in a time interval ΔT. In a process that remains stationary over ΔT, the Gutenberg-
Richter Parameters (GRP) a and b remain constant. Here, we use the time-dependent GRP to estimate
the Mean Recurrence Time (MRT) of volcanic earthquakes having or exceeding given magnitudes,
and thus the likelihood of major events occurring in the shorter time-scale (hours to days). The MRT

130   (t_T) between events with magnitude equal or greater than M may thus be estimated from Equation 1
as:

Equation 2 here

Increasing likelihood of major events may thus be estimated from the increasing rates of occur-
rence of smaller earthquakes. In practice this may prove to be a difficult task since the available

135   seismic catalogs frequently present completeness uncertainties derived from technical factors such
as the stability of the seismic networks and links, weather conditions, background noise, event count-
ing and magnitude assignment routines, among others. Problems of catalog completeness in general
mean an under-counting of the lowest magnitudes (Bell and Kilburn, 2012) that define a low-end
Magnitude Cutoff (MC) above which the GRL holds. A second major problem is that the evolution

140   of VT seismicity in the El Hierro crisis is highly variable, and the estimates for the GRL parameters
may vary in time and space, causing local distributions of shocks quite different from those of the
full catalog. This problem has been amply discussed in the literature about seismicity from different
origins (e.g. Wiemer et al, 1998; Lombardi, 2003; Marzocchi and Sandri, 2003; Helmstetter et al,
2007; Bengoubou-Valerius and Gibert, 2013; Alamilla et al, 2015; Márquez-Ramírez et al, 2015).

145   We have addressed those problems considering a moving and variable time-window ΔT in equa-
tions 1 and 2. In most cases, the time-window starts running when the cumulative energy released
by a VT swarm reaches the 10^{11}J energy threshold of Yokoyama (1988). Experience has shown that
at El Hierro such swarms precede a stage of accelerated seismicity with increasing magnitudes that
culminate in major (M>4) VT events.

150   The MRT algorithm starts a forecast when a swarm of at least 200 earthquakes with M≥1.5 are
detected in a time span of 5 days. Then, a completeness magnitude MC is calculated using the Max-
imum Curvature Method (MCM, Wiemer and Wyss, 2000). The GRL parameters are estimated for
each time-window using a Least-squares Regression Estimator (LRE) and/or a Maximum Likelihood
Estimator (MLE) (Peishan et al, 2003; Bengoubou-Valerius and Gibert, 2013). In general, the LRE

155   performs better for seismic swarms, as it allows the contribution of the dominant magnitudes of the
swarm to be emphasized underscoring only the linear part of the distribution. In successive swarms,
some patterns appear as the time to a mainshock approaches: MC may increase from the initial 1.5
to as much as 3 or more, and the time window shortens. Algorithm 1 shows a schematic description
(pseudocode) of the algorithm. The algorithm has been implemented in a batch processing mode that

160   may be activated every 24, 12 or 6 hours, depending on the level of activity.

Algorithm 1 near here

Table 1 shows the main features of the swarms detected at El Hierro, and Figure 5 shows the
evolution of the MRT for the initial four cycles of El Hierro activity. A warning window for the likely
occurrence of an earthquake exceeding M4 is issued when the calculated MRT for that magnitude

165   drops below 10 days, and a statement saying that there is an increased likelihood of an M4 (or higher)

earthquake in the following 10 days is delivered to the decision-makers. The warning remains active until the MRT returns to a value exceeding 10 days.

Figure 5 near here

Table 1 near here

170 An 8-month lull followed those four cycles, and as frequently happens, a belief that the seismo-volcanic crisis had ended spread throughout the island's population. Additional factors, such as a particularly strong winter storm and the Christmas holidays, caused failures of the IGN official seismic network that translated into a rather incomplete seismic catalog. When a new seismic swarm began on 2013-12-20, the MRT could only be calculated using predominantly data from the IGEO-

175 CSIC seismic research network. Figure 6 shows the MRT evolution using magnitudes from both catalogs. On 2013-12-24 a new warning was issued communicating to decision-makers the increased likelihood of a M5 or larger earthquake occurring in the following days. On 2013-12-27, at 17:46:02 UTC, the largest earthquake of the entire episode, with magnitude 5.4, caused numerous landslides across the island, fortunately without casualties. It is interesting to note that no M4 earthquakes

180 occurred in this stage.

Figure 6 near here

3 Discussion and Conclusions

Earthquake forecasting is a problem that has been addressed in the past from various different perspectives. Significant advances were obtained after the introduction of complexity theory (Lorenz,

185 1963; Mandelbrot, 1977) and the development of predictive algorithms (Gabrielov et al, 1986; Molchan, 1990; Keilis-Borok, 1996; Turcotte, 1997). Currently, the need to implement operational short-term earthquake forecasting based on predictive and forecasting algorithms has been stated by Jordan et al (2011). The MRT is one of such algorithms, based on a property that is typical of complex systems: seismic events cluster according to a simple scaling law, the Gutenberg-Richter

190 relationship (Equation 1). This empirical relationship contains information about the occurrence of large magnitudes embedded in the number of small-magnitude events (Helmstetter et al, 2007), and the time variations of the distribution of the small-magnitude events provides information about the time-scale of large-magnitude occurrences. In the case of VT earthquakes, two additional factors help to simplify the forecasting process: one is the limited geographic extent of the volcanic source

195 of seismicity, confining the spatial extension of the forecast. The other factor is the short time-scale, measured in days, at which orderly fluctuations of the GRPs evolve reflecting stress accumulations induced by the magma injections, and allowing rapid recognition of significant changes of the MRT as defined in Equation 2, and therefore viable short-term forecasts (García et al, 2014a). In contrast, a similar method for tectonic earthquakes would require recognizing orderly evolution patterns of the

Natural Hazards
and Earth System
Sciences
Discussions

Open Access

EGU

200 GRPs over times scales of years to decades, making short-term forecasting non-viable (e.g. Jordan et al, 2011).

We envision the El Hierro process as the result of magma injections causing stress distributions capable of triggering seismic swarms. Such swarms culminate with mainshocks that release stress concentrations, and are thus not followed by aftershock sequences. Further magma migrations cause

205 new swarms and mainshocks, in repeating, but non-periodic cycles of activity. For example, the largest earthquakes of the March and December 2013 swarms (see Table 1), were located at less than 20 km West from the westernmost shore of the island, suggesting a nearby localized stress source possibly resulting from subsurface magma injections under that region (Figure 7). From the initial stage of unrest in July 2011, five earthquake swarm cycles have been identified, but only the

210 first of these culminated in an eruption. The subsequent cycles show two main features: first, the swarms are separated by increasingly longer lull intervals, and second, they tend to culminate in mainshocks of increasing magnitudes (see Figure 2).

Figure 7 near here

The forecasting algorithm we are proposing here is based on the above-mentioned envisioning

215 of the process that is causing the seismic swarms, and begins when the background seismic energy exceeds the 10^{11}J energy threshold criterion of Yokoyama (1988). The acceleration of the earthquake rate (Figure 4-D) is interpreted in terms of piecewise estimations of the Gutenberg Richter parameters, The variations of those parameters are, in turn, translated as time-windows of increased likelihood of a large-magnitude earthquake. The MRT algorithm may be, and has been, used in real

220 time. In the absence of swarms, the GRPs are calculated with a long database of the seismic catalog, and updated on a daily basis (Algorithm 1), usually yielding fluctuating, but always very long values of the MRT (that may exceed 106 days). At the onset of a seismic swarm, the MRT drops rapidly to values of the order of 103 days. When this happens the GRPs are calculated from shorter time-windows of variable duration, provided that they contain a large enough number of events (at

225 least 200) to yield stable values of the GRPs. When the MRT for events of magnitude 4 or higher is less than 10 days, a warning is issued to the decision makers, expressed as a 10-day window of increased likelihood for larger, potentially damaging earthquakes. Up to the time of this submission, all the recent earthquakes of M≥4 at El Hierro have been forecasted several days in advance. Application of the MRT to other volcanoes may be relatively simple to implement, provided that the

230 observed seismicity corresponds to swarms of type D (Figure 4): increasing number of VT events with increasing magnitudes followed by a mainshock, and by a rapid decay of the seismicity afterwards. The algorithm may be readily adapted to any real-time monitoring system. In addition, the concept of time-windows for the increased likelihood of a large-magnitude earthquake should be easily understood and accepted by governmental decision-makers, making the management of risk

235 more effective.

Natural Hazards
and Earth System
Sciences

Open Access

EGU

Discussions

Natural Hazards
and Earth System
Sciences

Open Access

EGU

Discussions

References

Alamilla JL, Vai R, Esteva L (2015) Completeness assessment of earthquake catalogues under uncertain knowledge. J Seismolog 19(1):27–40, doi:10.1007/s10950-014-9448-x

Ancochea E, Hernán F, Cendrero A, Cantagrel JM, Fúster JM, Ibarrola E, Coello J (1994) Constructive and destructive episodes in the building of a young Oceanic Island, La Palma, Canary Islands, and genesis of the Caldera de Taburiente. J Volcanol Geotherm Res 60(3-4):243–262, doi:10.1016/0377-0273(94)90054-X

Bell AF, Kilburn CR (2012) Precursors to dyke-fed eruptions at basaltic volcanoes: insights from patterns of volcano-tectonic seismicity at Kilauea volcano, Hawaii. Bull Volcanol 74(2):325–339, doi:10.1007/s00445-011-0519-3

Bengoubou-Valerius M, Gibert D (2013) Bootstrap determination of the reliability of b-values: an assessment of statistical estimators with synthetic magnitude series. Nat Hazards 65(1):443–459, doi:10.1007/s11069-012-0376-1

Benoit JP, McNutt SR (1996) Global volcanic earthquake swarm database 1979-1989. Open-file report 96-69, US Department of the Interior, US Gological Survey

Brumbaugh D, Hodge B, Linville L, Cohen A (2014) Analysis of the 2009 earthquake swarm near Sunset Crater volcano, Arizona. J Volcanol Geotherm Res 285:18–28, doi:10.1016/j.jvolgeores.2014.07.016

Carracedo JC, Day SJ, Guillou H, Pérez-Torrado FJ (1999) Giant Quaternary landslides in the evolution of La Palma and El Hierro, Canary Islands. J Volcanol Geotherm Res 94:169–190, doi:10.1016/S0377-0273(99)00102-X

De la Cruz-Reyna S, Yokoyama I, Martinez-Bringas A, Ramos E (2008) Precursory seismicity of the 1994 eruption of Popocatepetl Volcano, Central Mexico. Bull Volcanol 70(6):753–767, doi:doi:10.1007/s00445-008-0195-0

Del Pezzo E, Bianco F, Saccorotti G (2003) Duration magnitude uncertainty due to seismic noise: inferences on the temporal pattern of GR b-value at Mt. Vesuvius, Italy. Bull Seismol Soc Am 93(4):1847–1853, doi:10.1785/0120020222

Farrell J, Husen S, Smith RB (2009) Earthquake swarm and b-value characterization of the Yellowstone volcano-tectonic system. J Volcanol Geotherm Res 188(1):260–276, doi:10.1016/j.jvolgeores.2009.08.008

Gabrielov A, Dmitrieva O, Keilis-Borok V, Kossobokov V, Kutznetsov I, Levshina T, Mirzoev K, Molchan G, Negmatullaev S, Pisarenko V, Prozorov A, Rinheart W, Rotwain I, Shelbalin P, Shnirman M, Schreider S (1986) Algorithms of long-term earthquakes' prediction, international school on research oriented to earthquake prediction–algorithms, software and data handling edn. Centro Regional de Sismología para América del Sur, Lima, Peru

García A, Berrocoso M, Marrero JM, Fernández-Ros A, Prates G, De la Cruz-Reyna S, Ortiz R (2014a) Volcanic Alert Level System (VALS) developed during the (2011-2013) El Hierro (Canary Island) volcanic process. Bull Volcanol 76:825, doi:10.1007/s00445-014-0825-7

García A, Fernández-Ros A, Berrocoso M, Marrero J, Prates G, De la Cruz-Reyna S, Ortiz R (2014b) Magma displacements under insular volcanic fields, applications to eruption forecasting: El Hierro, Canary Islands, 2011?2013. Geophys J Int 196:1–13, doi:10.1093/gji/ggt505

Gee MJ, Watts AB, Masson DG, Mitchell NC (2001) Landslides and the evolution of El Hierro in the Canary Islands. Mar Geol 177(3-4):271–293

Gutenberg B, Richter CF (1944) Frequency of earthquakes in California. B Seismol Soc Am 34:185–188

Helmstetter A, Kagan YY, Jackson DD (2007) High-resolution time-independent grid-based forecast for M 5 earthquakes in California. Seismological Research Letters 78(1):78–86, doi:10.1785/gssrl.78.1.78

285 Hurst T, Jolly AD, Sherburn S (2014) Precursory characteristics of the seismicity before the 6 August 2012 eruption of Tongariro volcano, North Island, New Zealand. J Volcanol Geotherm Res 286:294–302, doi:10.1016/j.jvolgeores.2014.03.004

Ibáñez JM, De Angelis S, Díaz-Moreno A, Hernández P, Alguacil G, Posadas A, Pérez N (2012) Insights into the 2011-2012 submarine eruption off the coast of El Hierro (Canary Islands, Spain) from statistical analyses

290 of earthquake activity. Geophys J Int 191(2):659–670, doi:10.1111/j.1365-246X.2012.05629.x

Jordan TH, Chen YT, Gasparini P, Madariaga R, Main I, Marzocchi W, Papadopoulos G, Sobolev G, Yamaoka K, Zschau J (2011) Operational Earthquake Forecasting. State of Knowledge and Guidelines for Utilization. Ann Geophys-Italy 54(4):315–391, doi:10.4401/ag-5350

Keilis-Borok V (1996) Intermediate-term earthquake prediction. Proc Natl Acad Sci USA 93(9):3748–3755

295 Leahy GM, Collins JA, Wolfe CJ, Laske G, Solomon SC (2010) Underplating of the Hawaiian Swell: evidence from teleseismic receiver functions. Geophys J Int 183(1):313–329, doi:10.1111/j.1365-246X.2010.04720.x

Lombardi AM (2003) The maximum likelihood estimator of b-value for mainshocks. Bull Seismol Soc Am 93(5):2082–2088, doi:10.1785/0120020163

López C, Blanco MJ, Abella R, Brenes B, Rodríguez-Cabrera VM, Casas B, Cerdeña ID, Felpeto A, de Vil-

300 lalta F, del Fresno C, García O, García-Arias M, García-Cañada L, Gomis-Moreno A, González-Alonso E, Guzmán-Pérez J, Iribarren I, López-Díaz R, Luengo-Oroz N, Meletlidis S, Moreno M, Moure D, Pereda de Pablo J, Rodero C, Romero E, Sainz-Maza S, Sentre-Domingo M, Torres P, Trigo P, Villasante-Marcos V (2012) Monitoring the volcanic unrest of El Hierro (Canary Islands) before the onset of the 2011-2012 submarine eruption. Geophys Res Lett 39:L13,303, doi:10.1029/2012GL051846

305 Lorenz EN (1963) Deterministic nonperiodic flow. J Atmos Sci 20(2):130–141

Mandelbrot BB (1977) Fractals: Form, Chance and Dimension. W. H. Freeman and Co.

Márquez-Ramírez V, Nava F, Zúñiga F (2015) Correcting the Gutenberg–Richter b-value for effects of rounding and noise. Earthquake Science 28(2):129–134, doi:10.1007/s11589-015-0116-1

Martínez-Arevalo C, Mancilla FdL, Helffrich G, García A (2013) Seismic Evidence of a Re-

310 gional Sublithospheric Low Velocity Layer beneath the Canary Islands. Tectonophysics 608:586–599, doi:10.1016/j.tecto.2013.08.021

Marzocchi W, Sandri L (2003) A review and new insights on the estimation of the b-valueand its uncertainty. Ann Geophys-Italy 46(6):1271–1282

Masson D, Watts A, Gee M, Urgeles R, Mitchell N, Bas TL, Canals M (2002) Slope failures on the flanks of

315 the western Canary Islands. Earth-Sci Rev 57(1-2):1–35

McLeod P, Sparks RSJ (1998) The dynamics of xenolith assimilation. Contrib Mineral Petr 132(1):21–33, doi:10.1007/s004100050402

Molchan G (1990) Strategies in strong earthquake prediction. Phys Earth Planet In 61(1-2):84–98, doi:10.1016/0031-9201(90)90097-H

320 Ogata Y (1992) Detection of precursory relative quiescence before great earthquakes through a statistical model. J Geophys Res-Sol Ea 97(B13):19,845–19,871, doi:10.1029/92JB00708

Peishan C, Tongxia B, Baokun L (2003) The b-Value and Earthquake Occurrence Period. Chinese Journal of
Geophysics 46(4):736–749, doi:10.1002/cjg2.3393

Portnyagin M, Almeev R, Matveev S, Holtz F (2008) Experimental evidence for rapid water ex-
325   change between melt inclusions in olivine and host magma. Earth Planet Sci Lett 272(3):541–552,
doi:10.1016/j.epsl.2008.05.020

Prates G, García A, Fernández-Ros A, Marrero JM, Ortiz R, Berrocoso M (2013) Enhancement of sub-daily
positioning solutions for surface deformation surveillance at El Hierro volcano (Canary Islands - Spain). Bull
Volcanol 75:724, doi:10.1007/s00445-013-0724-3

330 Stroncik N, Klügel A, Hansteen T (2009) The magmatic plumbing system beneath El Hierro (Canary Islands):
constraints from phenocrysts and naturally quenched basaltic glasses in submarine rocks. Contrib Mineral
Petr 157:593–607, doi:10.1007/s00410-008-0354-5

Turcotte DL (1997) Fractals and chaos in geology and geophysics. Cambridge University Press

Utsu T, Ogata Y (1995) The centenary of the Omori formula for a decay law of aftershock activity. J Phys Earth
335   43(1):1–33

Wiemer S, Wyss M (2000) Minimum magnitude of completeness in earthquake catalogs: examples from Alaska,
the western United States, and Japan. Bull Seismol Soc Am 90(4):859–869, doi:10.1785/0119990114

Wiemer S, McNutt SR, Wyss M (1998) Temporal and three-dimensional spatial analyses of the
frequency–magnitude distribution near Long Valley Caldera, California. Geophys J Int 134(2):409–421,
340   doi:10.1046/j.1365-246x.1998.00561.x

Yokoyama I (1988) Seismic energy releases from volcanoes. Bull Volcanol 50:1–13, doi:10.1007/BF01047504

Zobin VM (2001) Seismic hazard of volcanic activity. J Volcanol Geotherm Res 112(1):1–14,
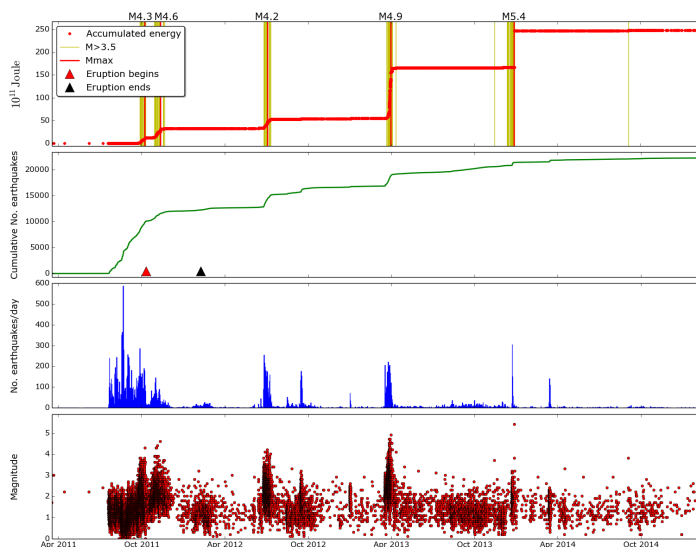doi:10.1016/S0377-0273(01)00230-X

FIGURES

Figure 1. Evolution of the seismic activity at El Hierro Island between 2011-03-18 and 2015-02-12. Data are from the IGN public earthquake catalog and the IGEO-CSIC seismic research network.
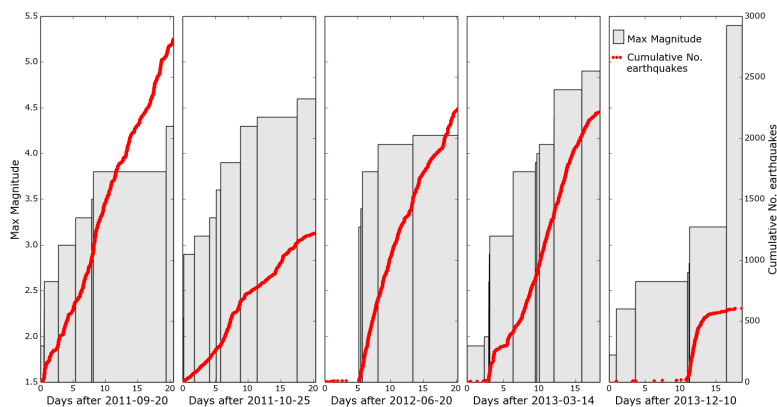

Figure 2. Time evolution of the daily count of VT events (red dots) and maximun magnitudes (gray bars) during the earthquake swarms of the El Hierro seismo-volcanic process.
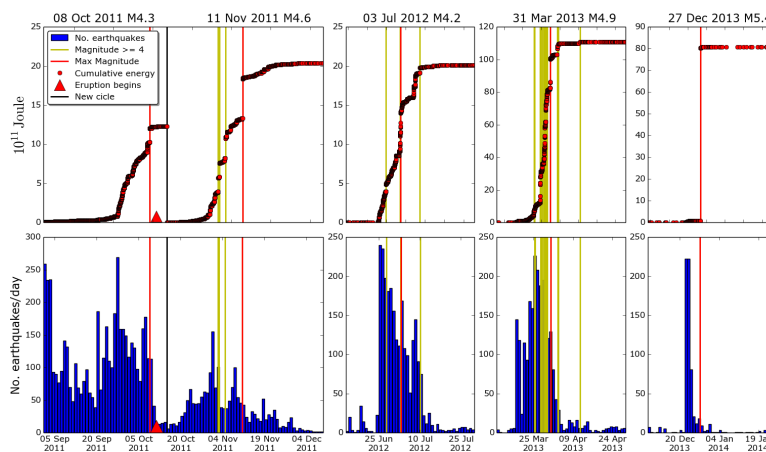
Figure 3. Seismo-volcanic crises identified at El Hierro Island (2011-2014). The upper plots show the evolution of seismic energy for each of the cycles of unrest. The lower plots show the daily event count. The plots illustrate how the seismic activity drops rapidly after the largest magnitude earthquakes. Particularly significant is the absence of aftershocks after the largest (M5.4) earthquake of 2013-12-27. Data are from IGN public earthquake catalog and the IGEO-CSIC seismic research network.
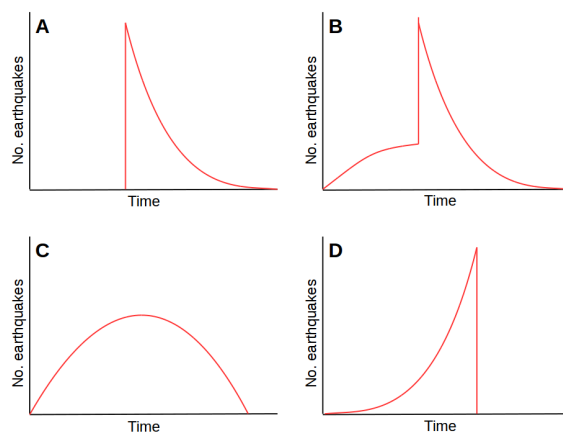

Figure 4. Seismic swarms are usually classified in three family types (A, B, C, Farrell et al, 2009; Brumbaugh et al, 2014). From our results at El Hierro in 2011-2015, we propose a fourth family type D, characterized by an increasing number of VT earthquakes and their magnitudes with time, and by a quick decay of the seismicity, in a matter of hours after a mainshock usually exceeding M4.
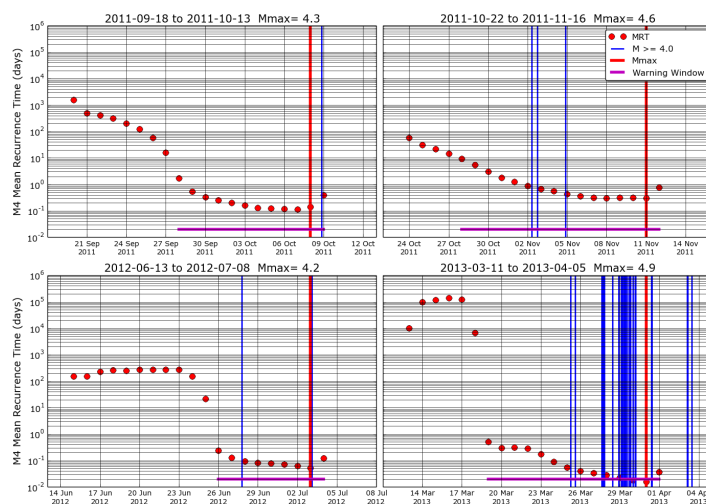
Figure 5. MRT evolution for four periods: 2011-08-18 to 2011-10-10; 2011-10-22 to 2011-11-13; 2012-06-13 to 2012-07-05; and 2013-03-11 to 2013-04-02. The warning windows were triggered when MRT dropped below 10 days.
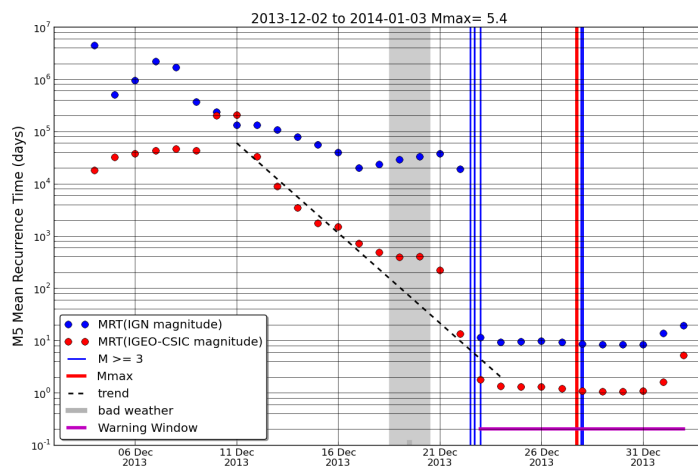

Figure 6. MRT evolution in December 2013 calculated from the IGN official catalog (blue) and from the IGEO-CSIC catalog (red). The magnitude of the earthquake on 2013-12-27 17:46:02 was estimated by IGN as 5.1, and as 5.4 by the IGEO-CSIC network and other international catalogs.
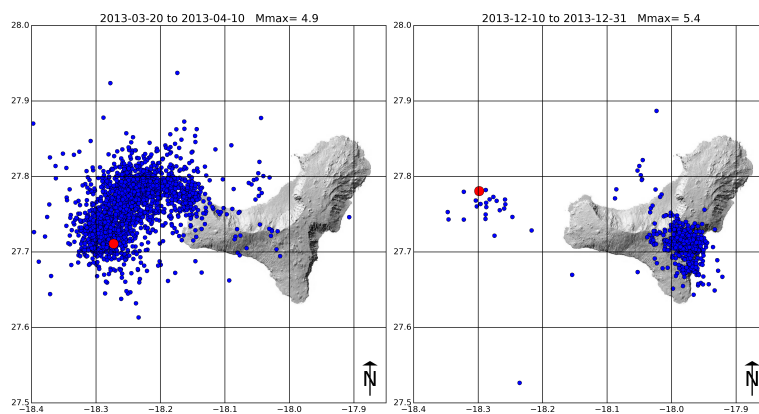
Natural Hazards
and Earth System
Sciences

Open Access

EGU

Discussions

Figure 7. Swarms and mainshock epicentres of the March and December 2013 seismicity cycles. The M5.4 mainshock of 2013-12-27, at 17:46:02 UTC is located in the same region of the March 2013 cycle.

Natural Hazards
and Earth System
Sciences
Discussions
Open Access
EGU

345   TABLES

Table 1. Characteristics of El Hierro swarms.

Mainshock Date	Magnitude		Swarm duration (days)	Number of events
	Mean	Max		
2011-10-08	2.33	4.3	10	934
2011-11-11	2.27	4.6	8	354
2012-07-03	2.35	4.2	5	635
2013-03-31	2.75	4.9	4	651
2013-12-27	2.09	5.4	4	466

EQUATIONS

$$\log[N(M)/\Delta T] = a - bM \tag{1}$$

$$t_T = \Delta T * 10^{[bM-a]} \tag{2}$$

Natural Hazards
and Earth System
Sciences

Open Access

Discussions

EGU

350   ALGORITHM

Algorithm 1 Pseudocode of the MRT algorithm developed to forecast mainshocks applied during the El Hierro seismo-volcanic process (2011-2015).

1: *Get seismic catalog* ← download from IGN website

2: *Count numer of events* ← In the last 5 days

3: **if** *earthquakes M1.5 > 200 events* **then**

4:    *Compute current MC* ← Magnitude Cutoff, using Maximum

5:    Curvature Method (MCM)

6:    *Compute Time window* ← Use constant MC

7:    *Compute number of events where M>MC*

8:    **if** *Number of events (M>MC) > 200 events* **then**

9:       *Select all events where M>MC*

10:      *Compute Gutenberg-Richter Parameters* ← Using Least-squares

11:      Regression Estimator (LRE) and/or

12:      Maximum Likelihood Estimator (MLE)

13:      *Compute Mean Recurrence Time (MRT) for M4 events*

14:      **if** *MRT for M4 events < 10 days* **then**

15:         **Activate Warning Window**

16:      **end if**

17:   **end if**

18: **end if**